2005-08-11

Solid-state current amplifier based on impact ionization

Aaron R. Hawkins
hawkins@ee.byu.edu

Hong-Wei Lee

Original Publication Citation

Lee, Hong W. and Aaron R. Hawkins. "Solid-state current amplifier based on impact ionization." Applied Physics Letters 87 (25)

Solid-state current amplifier based on impact ionization

Hong-Wei Lee and Aaron R. Hawkins
Department of Electrical and Computer Engineering, Brigham Young University, 459 Clyde Building, Provo, Utah 84602

(Received 22 April 2005; accepted 30 June 2005; published online 11 August 2005)

The operation principle, fabrication, and measurement results for a stand-alone amplifier based on impact ionization are reported. The device was built in silicon using standard microelectronic processes. Testing was performed by connecting the device to both silicon and indium-gallium-arsenide photodiodes to demonstrate its compatibility with arbitrary current sources. Preamplified leakage currents of less than 1 nA were measured along with current gains greater than 100. © *2005 American Institute of Physics*. [DOI: 10.1063/1.2031929]

The process of impact ionization in semiconductors has been well studied and quantified.[1] This phenomenon has been utilized to achieve current gain in a variety of semiconductor devices,[2,3] notably avalanche photodiodes[4] (APDs). APDs perform a dual function of converting photons into detectable electron-hole pairs and amplifying electrical current through impact ionization;[5] significant because APDs are able to achieve lower noise gain than transistor based amplifiers, especially for miniscule currents.[6] The characteristics of this gain mechanism (noise, voltage and temperature sensitivity, frequency response, etc.) vary greatly with different semiconductors and are dependent on ionization probabilities for both electrons and holes in a given material.[7,8] In general, silicon has the most desirable ionization properties of any semiconductor.[9] To this end, great lengths have been made to try and directly integrate silicon with other semiconductors to combine silicon's impact ionization mechanism with desirable physical properties of another semiconductor. APDs can again be cited as an example,[10,11] specifically those intended to utilize silicon gain regions and indium-gallium-arsenide (InGaAs) absorbing regions for near-infrared light collection.

In the context of the preceding paragraph, this letter presents a stand-alone amplifier based on the impact ionization gain mechanism. This device is designed to operate in conjunction with an independent current source with the two linked together only with a current conducting wire. This design differs from past implementation of semiconductor devices utilizing impact-ionization gain in that those devices were integrated on the same substrate and essentially required a current-generating region and an amplification region to be intimately connected. Any junction between these regions also must be depleted of mobile carriers to avoid recombination of carriers being injected from the current-generating region into the amplification region. The creation of a stand-alone impact ionization amplifier frees up these restrictions imposed upon device operation. Amplifier and current sources can be designed and optimized independently including using different semiconductors for each function without concern for lattice matching, heterojunctions, or fabrication compatibility. The first clear application, and the one that has driven this development, is the integration of such an amplifier with an external photodiode current source. An attractive implementation is an amplifier made from silicon providing low-noise gain and connected to a photodiode constructed from a low band-gap semiconductor providing infrared light absorption. Such low band-gap semiconductors usually display poor impact ionization characteristics, although we note that several groups have made significant progress in improving these characteristics by investigating a number of material systems[12,13] or using very short gain region designs.[14] The combination of an optimized photodiode with an independent silicon ionization amplifier, however, promises ease of implementation and light detection sensitivities comparable with the best all-silicon APDs, but at optical wavelengths well above silicon's absorption cutoff.

The operation principle of the impact ionization amplifier presented here is based on establishing a high electric field region vertically into a semiconductor and then injecting carriers horizontally into this region. The specific incarnation we have fabricated uses reverse-biased N^+-P^--P^+ doping regions in silicon to establish the necessary electric field. An external current source is then connected to a Schottky metal-semiconductor contact to the side of the high-field region. This amplifier is then a three-terminal device. Figure 1 illustrates its essential features with a photodiode represented as the current source. In operation, the highly doped P^+ substrate is grounded and a negative voltage in relation to this ground is applied to the photodiode, reverse biasing it. A contact to the heavily doped N^+ region is then biased positively in relation to ground. As this voltage is increased, the electric field increases between the N^+ region and the grounded substrate in the vertical direction. Increasing voltage also increases the depletion width in the P^- semiconduc-

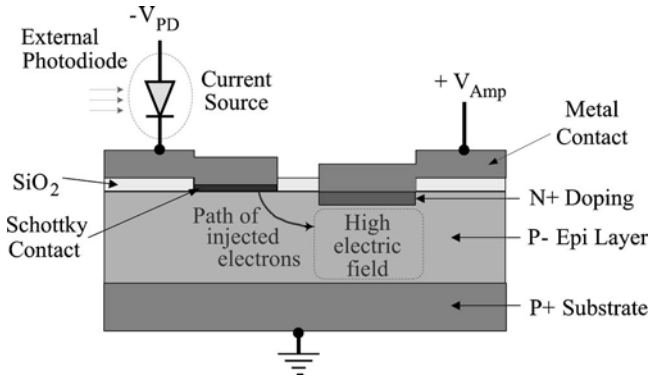

FIG. 1. Cross-sectional view of the impaction ionization amplifier illustrating its operation principle. A reverse-biased photodiode is connected as a current source. The high electric field is created by reverse biasing the N^+-P^--P^+ layers vertically.

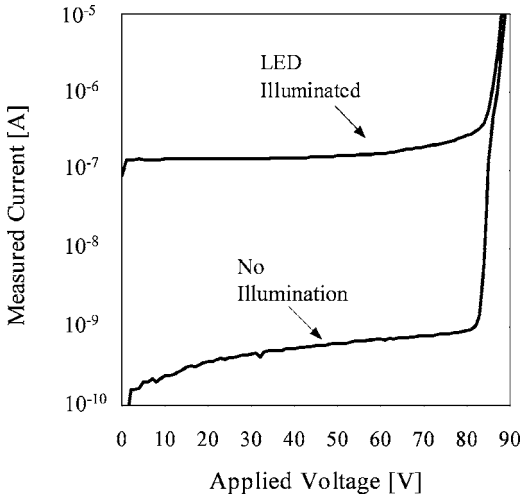

FIG. 2. Avalanche breakdown characteristics of the N^+-P^--P^+ gain region of the impact ionization amplifier with and without 650-nm LED illumination.

tor in the horizontal direction surrounding the N^+ region. At a critical voltage, this depletion width reaches the Schottky contact. Electrons can be injected into this depletion region and consequently into the high vertical electric field. Significant to the correct operation of the amplifier is the choice of dopings for the P^- layer and spacing between the Schottky contact and N^+ region. Ideally, when the critical depletion voltage is reached, the vertical electric field in the N^+-P^--P^+ region is already near avalanche breakdown so as to create significant gain. Otherwise, if large voltage increases are still required for gain, there is a danger of producing avalanche breakdown between the Schottky contact and N^+ region along the top surface of the device, which is undesirable.

Key to the operation of the device is the simultaneous vertical and horizontal flows of electrons and holes and isolating the impact ionization gain process to the vertical direction. In this way, holes created during ionization are directed towards the P^+ substrate instead of back towards the current source, which would result in carrier recombination and gain suppression. The desire to avoid recombination also explains the use of the Schottky contact as an injection point as opposed to a doped semiconductor region.

Discrete amplifiers were fabricated using silicon wafers produced by Komatsu Corporation consisting of an approximately 3 Ω-cm *p*-type epitaxial layer grown approximately 4 μm thick on a 0.01 Ω-cm *p*-type substrate. A 300 nm layer of silicon dioxide was thermally grown on the surface in a tube furnace with an oxygen atmosphere. A 10×10 μm^2 window was opened in the oxide and phosphorous-doped spin on glass applied. The wafers were placed in a tube furnace for 90 min at 1000 °C to produce the highly doped N^+ region required for the device. It is estimated that this phosphorous doping layer extended 1 μm below the wafer's surface. After stripping off the spin on glass, another 3×1.5 μm^2 window was opened in the surface oxide and a 140-nm-thick nickel layer evaporated directly onto the silicon surface. The nickel was then patterned to cover only the window opening and served as the Schottky contact for the amplifier. The spacing between the Schottky contact and N^+ region was varied between 3 and 9 μm for different devices on the same substrate. A 700 nm layer of aluminum was then evaporated onto the surface and patterned to form both the contact to the N^+ silicon region and to the nickel layer. Finally, the wafer was annealed in a tube furnace with a forming gas (N_2/H_2) environment for 5 min at 425 °C to produce a low resistance contact between the aluminum and N^+ silicon region, as well as to produce a nickel silicide at the Schottky contact interface.

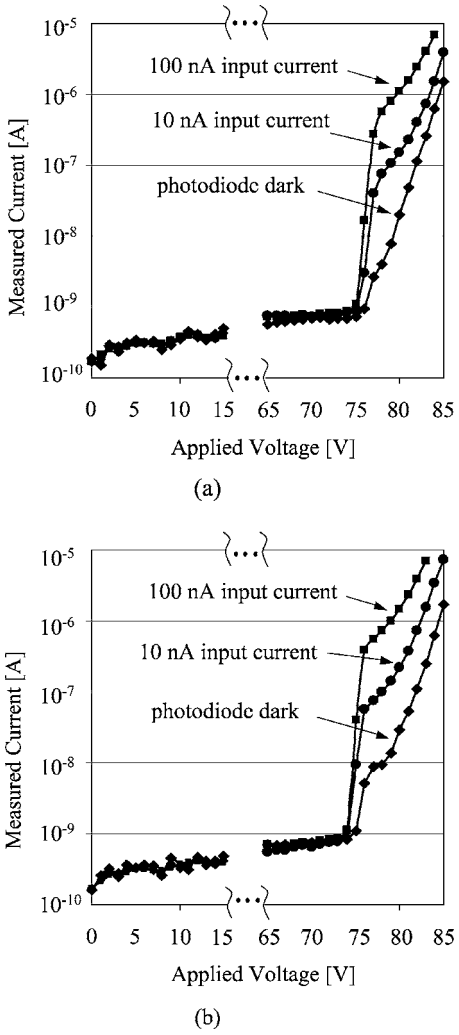

FIG. 3. Current vs voltage measurements at the N^+ region of the impact ionization amplifier when connected to external photodiode current sources. (a) Silicon photodiode illuminated with a white light source. (b) InGaAs photodiode illuminated with a 1.55-μm laser.

Completed amplifiers were tested using an HP4156 Parameter Analyzer and probe station. The first important parameter that was investigated was the impact ionization gain characteristics of the N^+-P^--P^+ gain region without an external current source connected to the device. This evaluation was done by connecting the P^+ substrate to ground and then applying positive voltage to the N^+ region though a microprobe. The device was then illuminated with a 650 nm wavelength light emitting diode to generate carriers near the top surface of the silicon. These carriers were then swept into the vertical high field region of the amplifier where they experienced impact ionization and produced current gain. The measured current versus voltage applied to the N^+ region is shown in Fig. 2. Plotted in this figure are the dark current for this structure (with no light shining on it) and the response to the light source. As can be seen, significant avalanche breakdown occurs beyond 85 V applied across the layers. Before this point however, current gain is evident in the light source

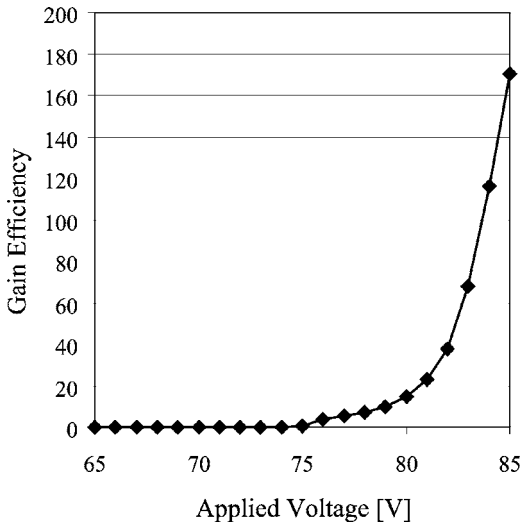

FIG. 4. Gain efficiency vs applied voltage at the N^+ region of the impact ionization amplifier with the 100-nA injection current from an external InGaAs photodiode.

response curve with a gain of about 3 near 85 V. The shape of this curve is very typical for silicon impact ionization and reminiscent of that produced by silicon *P-I-N* diodes. Although it is difficult to correlate gains for the side-injected fully operational amplifier with those produced from vertical optical injection, the latter do provide some indication of the gains that can be expected and provide evidence that the high-field gain region is operating as expected and with minimal dark (leakage) current.

Amplifiers were then evaluated when connected to external current sources, specifically photodiodes. Again an HP4156 Parameter Analyzer was used to bias the amplifier and photodiodes as shown in Fig. 1 with the connection between the photodiode and Schottky contact made using a microprobe and copper wire. Silicon and InGaAs photodiodes were used and the test results are summarized in Fig. 3. (The same amplifier was used to produce Figs. 2–4.) Figure 3(a) plots the current through the N^+ region of the amplifier versus voltage on the N^+ region when a silicon photodiode was connected and reversed biased to -20 V. A broadband white light source was used to illuminate the photodiode and produce the photocurrents indicated in the graphs. The photocurrent was measured directly through the voltage channel of the parameter analyzer biasing the photodiode. (Special care was taken to shield the silicon amplifier from the light source.) Figure 3(b) plots the amplifier current when connected to an InGaAs photodiode reversed biased to -4 V and illuminated with a 1.55 μm wavelength laser. As indicated in both plots in Fig. 3, at 75 V bias there is a large change in the current though the amplifier; this corresponds to the point where the depletion width out from the N^+ region reaches the Schottky contact (~ 5 μm in this case) and current can be injected horizontally into the high vertical electric field. Given the doping of the P^- layer and the voltage indicated on the figure, the calculated depletion width corresponds well to the known spacing between the Schottky contact and N^+ region. Although the response curves are not shown here, tests of amplifiers with different spacings between the Schottky contact and N^+ region revealed different depletion voltages that correlated with this spacing.

A critical figure of merit for this amplifier is its gain efficiency defined as gain efficiency = injection efficiency $\times$ current gain, where injection efficiency describes the percentage of carriers that are successfully injected from the current source into the amplifier and current gain is the multiplication factor of the injected current in the impact ionization gain region. To calculate gain efficiency from the plots in Fig. 3, dark current through the amplifier is subtracted from the total current when a photodiode is illuminated and the result is divided by the known photocurrent produced by the photodiode (as measured through the parameter analyzer). Figure 4 shows a plot of gain efficiency versus voltage on the amplifier when connected to the InGaAs photodiode producing 100 nA of current. The plots in Figs. 3 and 4 indicate that very high injection and gain efficiencies are possible for this amplifier.

The impact ionization amplifier described here opens up many new possibilities for improved device design and system performance, especially for optoelectronic communications and extreme sensitivity detection applications. Large numbers of these amplifiers could be fabricated on silicon substrates using processes compatible with current very large scale integrated circuit technology and also allowing for direct integration with subsequent transistor-based amplifier and logic circuitry. Beyond the initial demonstration described here, future work will include characterization of noise, temperature sensitivity, ac frequency response, and continued optimization for low leakage current operation.

The authors would like to acknowledge stimulating discussions and support from Mike Jack, Ken Kosai, and John Edwards at Raytheon Visions Systems in Goleta, CA.

[1] R. J. McIntyre, IEEE Trans. Electron Devices **46**, 1623 (1999).
[2] J. Kim, Y. Yamamoto, and H. H. Hogue, Appl. Phys. Lett. **70**, 2852 (1997).
[3] D. C. Herbert and R. G. Davis, IEEE Trans. Electron Devices **47**, 197 (2000).
[4] P. P. Webb, R. J. McIntyre, and J. Conradi, RCA Rev. **35**, 235 (1974).
[5] J. C. Campbell, A. G. Dentai, W. S. Holden, and B. L. Kasper, Electron. Lett. **19**, 818 (1983).
[6] F. Boudreau, Fiberoptic Product News **12**, 29 (1995).
[7] W. N. Grant, Solid-State Electron. **16**, 1189 (1973).
[8] C. A. Armiento and S. H. Groves, Appl. Phys. Lett. **43**, 198 (1983).
[9] A. R. Hawkins, W. Wu, and J. E. Bowers, Proc. SPIE **2999**, 68 (1997).
[10] A. R. Hawkins, T. E. Reynolds, D. R. England, D. I. Babic, M. J. Mondry, K. Streubel, and J. E. Bowers, Appl. Phys. Lett. **68**, 3692 (1996).
[11] Y. Kang, Y.-H. Lo, M. Bitter, S. Kristjansson, Z. Pan, and A. Pauchard, Appl. Phys. Lett. **85**, 1668 (2004).
[12] S. Miura, T. Mikawa, H. Kuwatsuka, N. Yasuoka, T. Tanahashi, and O. Wada, Appl. Phys. Lett. **54**, 2422 (1989).
[13] T. J. de Lyon, B. Baumgratz, G. Chapman, E. Gordon, A. T. Hunter, M. Jack, J. E. Jensen, W. Johnson, B. Johs, K. Kosai, W. Larsen, G. L. Olson, M. Sen, and B. Walker, Proc. SPIE **3629**, 256 (1999).
[14] J. C. Campbell, S. Demiguel, F. Ma, A. Beck, X. Guo, S. Wang, X. Zheng, X. Li, J. D. Beck, M. A. Kinch, A. Huntington, L. A. Coldren, J. Decobert, and N. Tscherptner, IEEE J. Quantum Electron. **10**, 777 (2004).